Ontogenetic Scaling of Theoretical Bite Force in Southern Sea Otters (*Enhydra lutris nereis*)

Chris J. Law[1,*]
Colleen Young[2]
Rita S. Mehta[1]
[1]Department of Ecology and Evolutionary Biology, University of California, 100 Shaffer Road, Santa Cruz, California 95060; [2]California Department of Fish and Wildlife, Marine Wildlife Veterinary Care and Research Center, 1451 Shaffer Road, Santa Cruz, California 95060

Accepted 6/29/2016; Electronically Published 8/18/2016

ABSTRACT

Sexual dimorphism attributed to niche divergence is often linked to differentiation between the sexes in both dietary resources and characters related to feeding and resource procurement. Although recent studies have indicated that southern sea otters (*Enhydra lutris nereis*) exhibit differences in dietary preferences as well as sexual dimorphism in skull size and shape, whether these intersexual differences translate to differentiation in feeding performances between the sexes remains to be investigated. To test the hypothesis that scaling patterns of bite force, a metric of feeding performance, differ between the sexes, we calculated theoretical bite forces for 55 naturally deceased male and female southern sea otters spanning the size ranges encountered over ontogeny. We then used standardized major axis regressions to simultaneously determine the scaling patterns of theoretical bite forces and skull components across ontogeny and assess whether these scaling patterns differed between the sexes. We found that positive allometric increases in theoretical bite force resulted from positive allometric increases in physiological cross-sectional area for the major jaw adductor muscle and mechanical advantage. Closer examination revealed that allometric increases in temporalis muscle mass and relative allometric decreases in out-lever lengths are driving these patterns. In our analysis of sexual dimorphism, we found that scaling patterns of theoretical bite force and morphological traits do not differ between the sexes. However, adult sea otters differed in their absolute bite forces, revealing that adult males exhibited greater bite forces as a result of their larger sizes. We found intersexual differences in biting ability that provide some support for the niche divergence hypothesis. Continued work in this field may link intersexual differences in feeding functional morphology with foraging ecology to show how niche divergence has the potential to reinforce sexual dimorphism in southern sea otters.

Keywords: biomechanics, cranial musculature, durophagy, feeding performance, Mustelidae, niche divergence, sexual dimorphism.

*Corresponding author; e-mail: cjlaw@ucsc.edu.

Physiological and Biochemical Zoology 89(5):347–363. 2016. 1522-2152/2016/8905-6037$15.00. DOI: 10.1086/688313

Introduction

Dietary specialization by some individuals within the same population is a prevalent phenomenon that is not well understood (Bolnick et al. 2011). The sex structure of populations introduces natural variability in morphology and behavior that may contribute to feeding differences between individuals. While sexual selection may drive morphological disparity between the sexes (Darwin 1871; Clutton-Brock 2007), natural selection may also select for traits that reduce competition for food resources (Darwin 1871; Hedrick and Temeles 1989; Shine 1989). The latter hypothesis is known as niche divergence and suggests that sexual dimorphism is linked to dietary partitioning (Darwin 1871). Sexual dimorphism attributed to niche divergence is often expressed as differences in cranial size and shape (Darwin 1871; Camilleri and Shine 1990; Radford and Plessis 2003; Thom and Harrington 2004), which further translates to differences in feeding performances between the sexes (Herrel et al. 1999, 2007; Bulté et al. 2008; McGee and Wainwright 2013; Thomas et al. 2015).

In many vertebrates, biting is the primary mechanism to capture, kill, and consume prey (Kardong 2014). Bite force, a widely used measure of feeding performance, has been shown to be a strong link between cranial morphology and dietary ecology (Herrel et al. 2007; Anderson et al. 2008; Bulté et al. 2008; Santana et al. 2010). Greater bite forces also strongly correlate with reduced handling times for both prey capture and consumption (Herrel et al. 2001; Verwaijen et al. 2002; van der Meij and Bout 2006; Anderson et al. 2008). In most cases, individuals with larger heads exert greater forces and can therefore expand their dietary breadth by consuming larger or more robust food items (Verwaijen et al. 2002; Herrel et al. 2006; Bulté et al. 2008). Therefore, by growth alone, both males and females exhibit increases in bite force that can lead to increased foraging efficiency and net energy intake (Binder and Valkenburgh 2000; Huber et al. 2006; Pfaller et al. 2011; Marshall et al. 2014).

The ability to generate large forces during feeding is particularly important for durophagous vertebrates, those that specialize on hard items such as bones, seeds, or shelled organisms

(Van Valkenburgh 2007; Collar et al. 2014). Unsurprisingly, a plethora of studies have revealed that bite force in durophagous species scales with positive allometry relative to body size through ontogeny (Erickson et al. 2003; Pfaller et al. 2011; Marshall et al. 2012; Kolmann et al. 2015). Ontogenetic increases in bite force can occur from a disproportionate increase in (1) head size (Anderson et al. 2008); (2) physiological cross-sectional area (PCSA) of the jaw adductor muscles, which can be altered by changing various components of muscle architecture including mass, pennation angle, and muscle fiber lengths (Pfaller et al. 2011; Kolmann et al. 2015); (3) mechanical advantage, which can be enhanced by shifting muscle insertion points or the bite point (Grubich 2005; Huber et al. 2008); or (4) any combination of the aforementioned changes (Hernandez and Motta 1997; Huber et al. 2006; Kolmann and Huber 2009). Although an increasing number of studies have examined the differential scaling of head size, jaw muscle force, mechanical advantage, and their contributions to bite force, few studies have examined these parameters in mammals (Santana and Miller 2016). Furthermore, even fewer studies have investigated whether scaling patterns of bite force and its underlying components differ between the sexes, particularly within mammals.

Southern sea otters (*Enhydra lutris nereis*) are an excellent mammalian system with which to examine scaling patterns of bite force and dimorphism in biting ability. These durophagous marine mustelids feed on a variety of hard-shelled invertebrates such as chitinous crabs and calcifying bivalves and gastropods (Riedman and Estes 1990). Like many durophagous mammals, sea otters exhibit several cranial adaptations that facilitate durophagy including short, blunt skulls (Riley 1985); taller and wider mandibular rami (Timm-Davis et al. 2015; bunodont dentition (Fisher 1941; Constantino et al. 2011); and fracture-resistant dental enamel (Ziscovici et al. 2014). Recent work on adult southern sea otters indicated that although size is the primary axis of craniomandibular variation, a handful of craniomandibular traits demonstrated significant shape differences between the sexes (Law et al., forthcoming). These size-corrected differences in jaw adductor muscle in-levers, cranial height, and postorbital constriction breadth suggest differences in biting ability between the sexes for a given body size.

In this study, we tested the hypothesis that the scaling patterns of muscle dissection–based estimations of bite force and the underlying anatomical components differ between the sexes. To test our hypothesis, we first investigated the anatomical traits that contribute to bite force generation in southern sea otters. We then simultaneously determined the scaling patterns of theoretical bite forces and skull components across ontogeny and assessed whether these scaling patterns differed between the sexes. Last, we elucidated which of these factors are responsible for the strong allometric patterns of bite force production.

Methods and Material

Specimens and Gross Dissections

We obtained 55 naturally deceased southern sea otters (24 females and 31 males; table A1) from the California Department of Fish and Wildlife (CDFW) Marine Wildlife Veterinary Care and Research Center from October 2013 to February 2016. The age class of each specimen was determined using a suite of morphological characteristics including total body length, tooth wear, and closure of cranial sutures (table A2; Hatfield 2006). Body mass was also measured for each specimen. All specimens stranded along the central California coast, within and throughout the current southern sea otter range (Pigeon Point in the north to Gaviota in the south).

We dissected the major jaw adductor muscles (superficial temporalis, deep temporalis, superficial masseter, deep masseter, and zygomaticomandibularis) following Scapino's (1968) cranial musculature description of various mustelids including the northern sea otter (*Enhydra lutris kenyoni*). While there was distinct separation between the superficial and deep temporalis, there was inadequate separation between the superficial masseter, deep masseter, and zygomaticomandibularis muscles (Scapino 1968). Therefore, we treated the three subdivisions as one muscle, the masseter (fig. 1*A*). Furthermore, because the medial pterygoid is positioned deep along the medial side of the mandible and cannot be excised intact, we did not include this muscle in our analyses. Muscles were removed from the left side of the skull, blotted dry, and weighed to the nearest 0.1 g using a digital scale.

We then measured the length and pennation angle of muscle fibers by digesting and separating the muscles in a solution of 15% aqueous nitric acid for 3–7 d depending on muscle size (Biewener and Full 1992). Muscle fiber lengths were measured to the nearest 0.01 mm using a digital caliper. Skulls were subsequently cleaned by a dermestid beetle colony at the California Academy of Sciences or with a maceration tank at CDFW. We then photographed and digitally measured the condylobasal length (distance from the anteriormost point on the premaxillae to the plane of the posterior surface of the occipital condyles), zygomatic breadth (greatest distance across the zygomatic arches), and cranial height (distance perpendicular to the palate plane from the lateralmost point of the mastoid process to the point of the sagittal crest directly superior to the mastoid process) of each cranium using ImageJ (Schneider et al. 2012; fig. 1*C*, 1*D*).

Bite Force Model

Because of its craniostylic characteristics, the mammalian jaw can be modeled as a static third-class lever where an axis passing through the temporomandibular joints (TMJs) serves as the fulcrum and muscle forces generated by jaw adductor muscle contractions create rotation of the lower jaw about this fulcrum (Davis et al. 2010). Under static lever equilibrium, the force of biting balances the rotation of the lower jaw created by these muscle forces (fig. 1*A*, 1*B*).

We first calculated PCSA for each muscle based on muscle mass (m), mean fiber length (f), muscle density (ρ), and fiber pennation angle (θ; Sacks and Roy 1982):

$$\text{PCSA} = \frac{m}{\rho}\frac{\cos[\theta]}{f}.$$

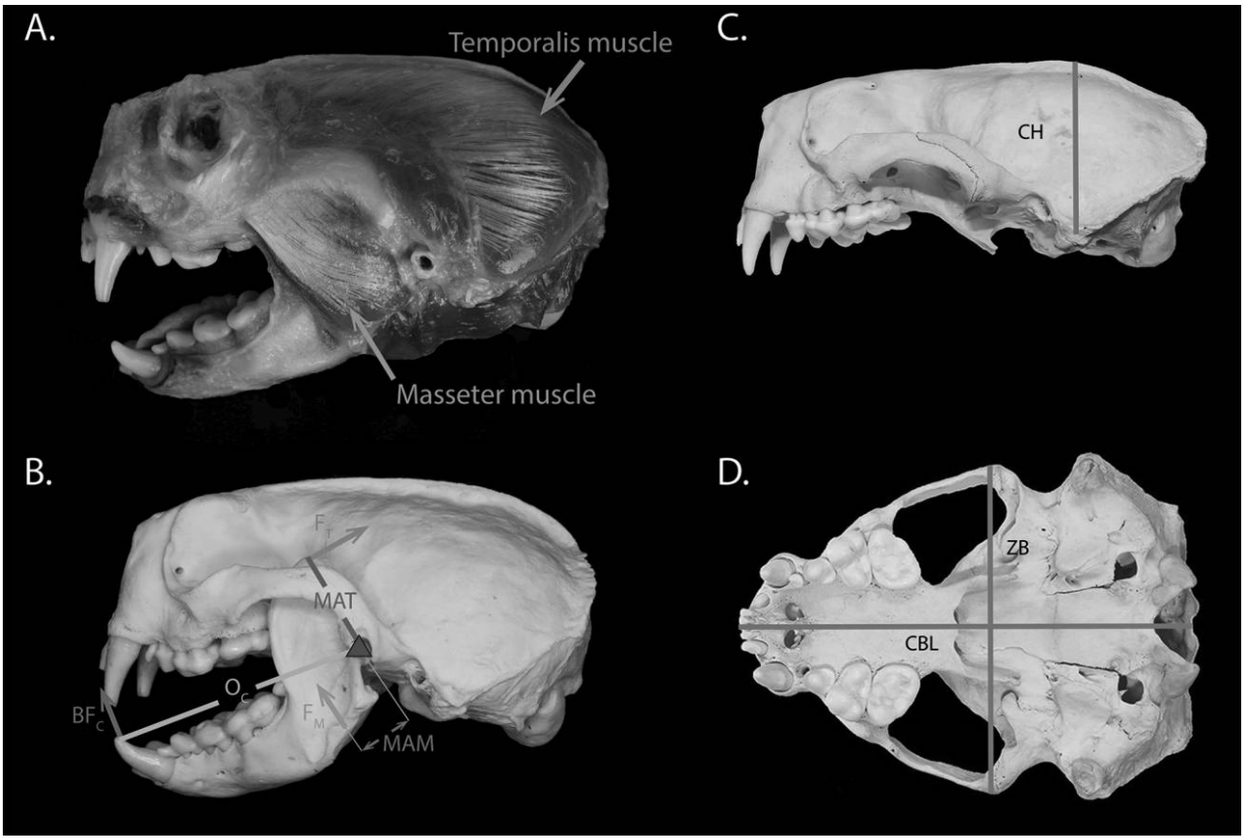

Figure 1. *A*, Photograph of the two major jaw adductor muscles of an adult male sea adult. *B*, Forces of the temporalis and masseter muscles (F_T and F_M) are applied at given distances (MAT and MAM) from the fulcrum (triangle), creating rotation of the lower jaw. Bite forces, at given distances (O_C and O_M), balance these muscle forces. Using the model $BF_X = 2[(F_T \times MAT + F_M \times MAM)/O_X]$, theoretical bite forces are calculated at the canine (BF_C) and the molar (BF_M). *C*, *D*, Cranial dimensions used in this study. CBL = condylobasal length; CH = cranial height; ZB = zygomatic breadth. A color version of this figure is available online.

We used a mammalian muscle density of 1.06 g/cm (Mendez and Keys 1960). Jaw muscle fibers were parallel; thus, we used a fiber pennation angle of 0°. PCSA of the temporalis muscle was totaled as a sum of the PCSA calculated for the superficial and deep temporalis subdivisions and modeled as a single muscle. To estimate muscle forces of the temporalis and masseter, we multiplied PCSA by a muscle stress value of 25 N/cm^2 (Herzog 1994), a value that is commonly used in other dissection-based estimations of bite force (Herrel et al. 2008; Davis et al. 2010; Santana et al. 2010; Pfaller et al. 2011). We then modeled each muscle force as a single force vector (F_T and F_M) and applied them to the insertion points of the temporalis, the top of the coronoid process of the mandible, and the masseter, the midpoint between the anteriormost edge of the masseteric fossa and the angular process of the mandible. Our estimation of muscle forces assumed that all of the jaw muscles were maximally activated.

We calculated maximum theoretical bite forces (BF_X) by adding the moment (product of the force vector and in-lever length) of each jaw adductor muscle, dividing by the out-lever, and multiplying by 2 to account for bilateral biting:

$$BF_X = 2\left(\frac{F_T \times MAT + F_M \times MAM}{O_X}\right),$$

where F_T and F_M are the force vectors of the temporalis and masseter, respectively; MAT is the perpendicular in-lever length of the temporalis, measured as the perpendicular distance from the temporalis muscle force vector to the TMJ; MAM is the perpendicular in-lever length of the masseter, measured as the perpendicular distance from the masseter muscle force vector to the TMJ; and O_X is the out-lever length, measured as the distance between the bite point and the TMJ (Davis et al. 2010). Muscle force vectors were estimated based on gape angle measured from the maxillary tip to the condyle to the mandibular tip. Because data for gape angles were unavailable for all age classes, we estimated maximum gape angle based on measurements from osteological specimens. We used constant gape angles of 45°, 55°, 60°, and 62° for pups, immatures, subadults, and adults, respectively. Our estimation of adult gape angles is similar to the mean gape angle range (66.5°) obtained from observational studies of adult sea otter feeding (Timm 2013). We calculated theoretical bite forces at two locations, the lower canine (BF_C) and in be-

Table 1: Scaling of cranial dimensions against body mass and body length

	Sex effects		Scaling relationships				
	Intercept	*P*	R^2	Slope (95% CI)	*P*	Isometric prediction	Scaling patterns
A. Cranial dimensions against BM:							
CBL	F 4.35, M 4.35	.679	.89	.17 (.15–.19)	**<.001**	.33	NA
ZB	F 4.02, M 4.05	.959	.9	.18 (.17–.20)	**<.001**	.33	NA
CH	F 3.81, M 3.74	.929	.65	.12 (.09–.13)	**<.001**	.33	NA
B. Cranial dimensions against BL:							
CBL	F 2.48, M 2.57	.051	.91	.53 (.49–.58)	**<.001**	1	NA
ZB	F 1.86, M 2.11	.195	.91	.57 (.52–.63)	**<.001**	1	NA
CH	F 2.72, M 2.43	.621	.57	.36 (.30–.42)	**<.001**	1	NA

Note. Cranial dimensions served as dependent variables, while body mass (BM; pt. A) and body length (BL; pt. B) served as independent variables. *P* values from tests of sex effects reflect differences in elevation between the sexes, and *P* values from tests of isometry reflect differences from isometric predictions. All *P* values are reported as Benjamini-Hochberg-corrected values. Bold *P* values indicate significance ($\alpha = 0.05$). See table A3 for tests in difference of slopes. CI = confidence interval. For scaling patterns, NA = negative allometry. CBL = condylobasal length; CH = cranial height; F = female; M = male; ZB = zygomatic breadth.

tween the first and second molars of the lower jaw (BF_M). These two bite points represent important bite positions in prey processing for sea otters; biting at the canine is used to pry open hard-shelled invertebrates such as bivalves, whereas the molars are used to crush items before consumption (Riedman and Estes 1990). All in-lever and out-lever measurements were taken from photographs of the lateral view of the mandible in ImageJ v. 1.48 (Schneider et al. 2012).

Statistical Analyses

We performed all statistical analyses in R 3.2.3 (R Core Team 2015). We natural log transformed (ln) all variables to reduce skewness and heteroscedasticity across values of all variables and ensure that traits exhibited linear relationships with each other. To determine which cranial dimension (condylobasal length, zygomatic breadth, cranial height) and body size metric (body mass, body length) were the best predictors of bite force, we performed separate sex-specific multiple regression analyses. In each analysis, we used theoretical bite force as the dependent variable and cranial dimensions and body size as the independent variables. Following Baliga and Mehta (2014), we estimated the R^2 decomposition of each model (Zuber and Strimmer 2011) by computing correlations between the response and the Mahalanobis-decorrelated predictors (CAR scores) using the R package relaimpo (Grömping 2006). Comparing these scores allowed us to assess the relative importance of each predictor, enabling us to identify which measurement most strongly predicted each sex's ontogenetic bite force trajectory.

We used the R package smatr (Warton et al. 2011) to simultaneously (1) examine scaling patterns between/within the body size, cranial dimensions, theoretical bite forces, and components of our bite force model and (2) assess whether these scaling patterns differed between the sexes. To examine scaling among body size and cranial dimensions, we performed standardized major axis (SMA) regressions with cranial dimensions as dependent variables, body mass and body length as independent variables, and sex as the main factor. Similarly, to examine scaling of bite force generation, we performed SMA regressions with theoretical bite forces, model components (in-levers, out-levers, jaw muscle masses, and muscle fiber lengths), mechanical advantage, and muscle PCSAs as dependent variables, body size and cranial dimensions as the independent variables, and sex as the main factor. In each independent analysis, we first tested the null hypothesis that the mean SMA regression slopes and elevation did not significantly differ between the sexes. Because we found nonsignificant differences between slopes in all of our analyses (see "Results"), we pooled the male and female data sets for subsequent scaling analyses. Scaling relationships between all SMA regression slopes were compared with null predictions of isometry (linear measurements = 1.0; areas and forces = 2.0; masses = 3.0), based on Euclidean geometry (Hill 1950; Schmidt-Nielsen 1984; Emerson and Bramble 1993). Using modified *t*-tests, we tested whether each slope significantly deviated from isometry (i.e., allometry). Predicted slopes significantly greater or less than the 95% confidence intervals of the observed SMA regression slopes were interpreted as positive or negative allometry, respectively. We adjusted all *P* values using a Benjamini-Hochberg correction to reduce the type I error probability across multiple comparisons (Benjamini and Hochberg 1995). We then ran a second set of sex-specific multiple regression analyses and calculated CAR scores to assess which component of the bite force model contributed the most to theoretical bite forces in each sex. In these analyses, we used theoretical bite force as the dependent variable and model components (out-levers, in-levers, jaw muscle masses, and jaw fiber length) as the independent variables.

Last, we used ANOVAs to test for sexual size differences of each trait and theoretical bite force in the adult specimens. We used only adults because differential dietary specialization between the sexes has been examined only in adult southern sea otters. We did not use natural log–transformed values for these ANOVA tests.

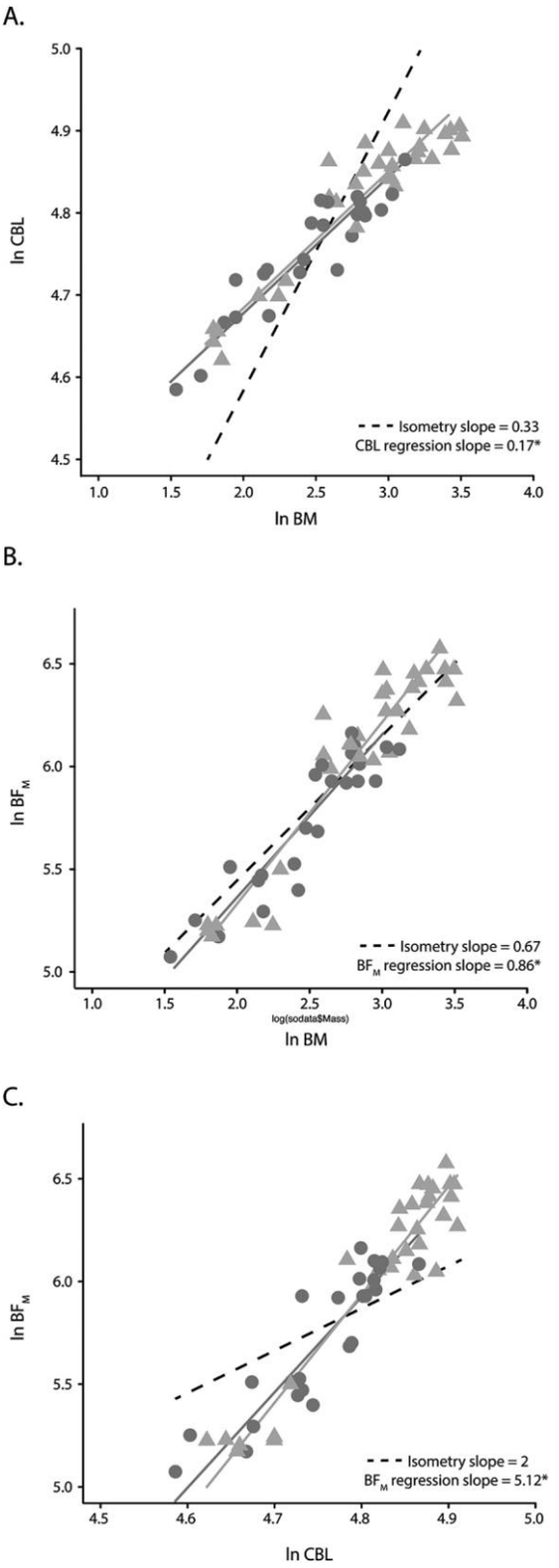

Figure 2. Scaling of condylobasal length (CBL) on body mass (BM) for female and male southern sea otters (*A*), bite force at the molar (BF_M) on condylobasal length (*B*), and bite force at the molar on body mass (*C*). Circles indicate female otters, and triangles indicate male otters. Dark gray and light gray solid lines represent standardized major axis regressions for females and males, respectively. Dotted lines indicate line of isometry. An asterisk indicates that the slope is significantly different from isometry. See tables 1, 2, and A3 for more details. A color version of this figure is available online.

Results

Mean slopes between the sexes were not significantly different in all SMA analyses (table A3), indicating that scaling patterns of cranial morphology and biting ability do not differ between females and males.

Scaling of Cranial Morphometrics

Condylobasal length, zygomatic breadth, and cranial height all scaled with negative allometry relative to body mass and body length (table 1; fig. 2*A*). Among cranial traits, zygomatic breadth scaled isometrically to condylobasal length ($b = 1$, $P = 0.153$), whereas cranial height scaled with negative allometry ($b < 1$, $P < 0.001$). These trends were observed in both males and females.

Scaling of Biting Biomechanics

Theoretical bite force at the canine and molar showed positive allometric relationships with body and cranial dimensions (table 2; fig. 2*B*, 2*C*). CAR scores indicated that ln condylobasal length and ln body mass were the greatest head and body predictors of theoretical bite force in both sexes (table 3).

All bite force model components, mechanical advantage at the canine, and muscle PCSA displayed positive allometry relative to ln condylobasal length (all $P \leq 0.001$–0.012; table 4; figs. 3, 4). However, we found no relationship between ln condylobasal length and mechanical advantage at the molar for both jaw muscles (table 4).

Conversely, disparate scaling patterns emerged when we examined the ontogeny of the bite force model components against ln body mass (table A4, pt. A). Ln lengths of the out-levers and temporalis in-lever scaled with negative allometry relative to ln body mass ($b < 0.33$, $P \leq 0.001$–0.041), whereas ln masseter in-lever length scaled isometrically ($b = 0.33$, $P = 0.408$). Masses of the jaw adductor muscles also differed in allometric scaling: ln temporalis mass scaled with positive allometry relative to ln body mass ($b > 1$, $P = 0.041$), and ln masseter mass scaled with negative allometry relative to ln body mass ($b < 1$, $P = 0.047$). Last, ln fiber lengths for both jaw adductor muscles scaled isometrically relative to ln body mass ($b = 0.33$, $P = 0.183$–0.578). Examination of mechanical advantage and PCSA against ln body mass also revealed disparate scaling patterns (table A4, pt. B, C). Ln temporalis and masseter mechanical advantage at the canine scaled with positive allometry ($b > 0$, both $P < 0.001$; table A4, pt. B). In contrast, there was no significant relationship between ln body mass and ln mechanical advantage at the molar for both jaw muscles ($R^2 = 0.00$–0.10, $P = 0.067$–0.561). Overall ln PCSA of the temporalis and of the masseter scaled with positive allometry ($b > 0.67$, $P < 0.001$) and isometry ($b = 0.67$, $P = 0.198$), respectively (table A4, pt. C).

Table 2: Scaling of estimated bite forces against body and cranial dimensions

	Sex effects		Scaling relationships				
	Intercept	*P*	R^2	Slope (95% CI)	*P*	Isometric prediction	Scaling pattern
A. BF_C against body and cranial dimensions:							
BM	F 3.03, M 2.71	.996	.88	.92 (.84–1.01)	**<.001**	.67	PA
BL	F −6.40, M −7.62	.297	.88	2.89 (2.63–3.18)	**<.001**	2	PA
CBL	F −18.90, M −22.49	.621	.9	5.47 (5.02–5.96)	**<.001**	2	PA
ZB	F −14.54, M −18.87	.959	.9	4.98 (4.56–5.44)	**<.001**	2	PA
CH	F −29.85, M −26.69	.929	.61	8.06 (6.79–9.57)	**<.001**	2	PA
B. BF_M against body and cranial dimensions:							
BM	F 3.77, M 3.55	.831	.89	.86 (.78–.95)	**<.001**	.67	PA
BL	F −5.15, M −5.94	.130	.87	2.61 (2.33–2.91)	**<.001**	2	PA
CBL	F −16.97, M −19.61	.929	.89	5.12 (4.368–5.59)	**<.001**	2	PA
ZB	F −12.85, M −16.29	.929	.89	4.66 (4.25–5.11)	**<.001**	2	PA
CH	F −27.33, M −23.48	.996	.62	7.46 (6.30–8.84)	**<.001**	2	PA

Note. Bite force at the canine (BF_C; pt. A) and molar (BF_M; pt. B) served as dependent variables, while body and cranial dimensions served as independent variables. *P* values from tests of sex effect reflect differences in elevation between the sexes, and *P* values from tests of isometry reflect differences from isometric predictions. All *P* values are reported as Benjamini-Hochberg-corrected values. Bold *P* values indicate significance ($\alpha = 0.05$). See table A3 for tests in difference of slopes. For scaling patterns, PA = positive allometry. BM = body mass; BL = body length; CBL = condylobasal length; CH = cranial height; F = female; M = male; ZB = zygomatic breadth.

CAR scores revealed that out of the seven components in our bite force model, the temporalis muscle mass was the greatest contributor to theoretical bite force in both sexes (table 5). A second CAR score analysis also found that temporalis muscle mass contributed to the bite force model more than mechanical advantage (table A5).

Effects of Sexual Dimorphism on the Ontogeny of Biting Biomechanics

Mean slopes between the sexes were not significantly different in all SMA analyses (table A3). In addition, we did not find significant elevation effects between the sexes in our SMA regressions of cranial dimensions against body size metrics (table 1; fig. 2*A*) or theoretical bite forces against body size and cranial dimensions (table 2; fig. 2*B*, 2*C*). However, SMA regressions of the bite force model components against body mass and condylobasal length revealed significant elevation effects in some model components (tables 4, A4; fig. 4). These analyses suggested that for a given condylobasal length or body mass, female sea otters exhibit relatively longer temporalis and masseter in-levers but shorter molar out-levers (tables 4A, A4, pt. A; fig. 4). In addition, overall temporalis and masseter mechanical advantage to the canine was relatively higher in females than in males (tables 4, pt. B; A3).

Adult Characteristics

Males were significantly larger than females for absolute values of body size and cranial dimensions ($P = 0.001$–0.013; table 6).

Table 3: Multiple regression analyses of morphological predictors of estimated bite force

	CAR scores for BF_C								
	BM	BL	CBL	ZB	CH	Adjusted R^2	*F* ratio	df	*P*
Female	**.301**	.260	**.217**	.143	.026	.93	54.32	5, 25	**<.001**
Male	**.283**	.147	**.296**	.119	.097	.93	55.75	5, 18	**<.001**
	CAR scores for BF_M								
	BM	BL	CBL	ZB	CH				
Female	**.299**	.273	**.212**	.132	.021	.92	44.5	5, 25	**<.001**
Male	**.281**	.160	**.276**	.108	.110	.92	48.41	5, 18	**<.001**

Note. Bold correlation-adjusted correlation (CAR) scores represent the best body and cranial predictors of estimated bite force at the canine (BF_C) and at the molar (BF_M). Bold *P* values indicate significance ($\alpha = 0.05$). BM = body mass; BL = body length; CBL = condylobasal length; CH = cranial height; ZB = zygomatic breadth.

Table 4: Scaling of bite force model components (pt. A), mechanical advantage (pt. B), and physiological cross-sectional area against condylobasal length (CBL; pt. C)

	Sex effects		Scaling relationships				
	Intercept	*P*	R^2	Slope (95% CI)	*P*	Isometric prediction	Scaling patterns
A. BF components against CBL:							
O_C	F −3.75, M −3.21	.057	.94	1.09 (1.02–1.16)	**.012**	1	PA
O_M	F −6.37, M −6.47	**.000**	.93	1.58 (1.45–1.72)	**<.001**	1	PA
MAT	F −8.14, M −7.59	**.000**	.89	1.74 (1.59–1.91)	**<.001**	1	PA
MAM	F −8.09, M −9.39	**.000**	.67	1.87 (1.59–2.18)	**<.001**	1	PA
m_{TEM}	F −25.89, M −30.85	.959	.92	6.81 (6.31–7.36)	**<.001**	3	PA
m_{MAS}	F −22.18, M −25.36	.228	.88	5.33 (4.83–5.86)	**<.001**	3	PA
f_{TEM}	F −10.10, M −8.85	.610	.64	2.15 (1.83–2.54)	**<.001**	1	PA
f_{MAS}	F −8.65, M −8.15	.056	.4	1.83 (1.48–2.26)	**<.001**	1	PA
B. MA against CBL:							
$temMA_C$	F −4.93, M −4.98	**.002**	.56	.77 (.64–.92)	**<.001**	0	PA
$temMA_M$			NS				
$masMA_C$	F −6.40, M −7.33	**.000**	.17	1.05 (.79–1.39)	**<.001**	0	PA
$masMA_M$			NS				
C. PCSA against CBL:							
$PCSA_{TEM}$	F −20.13, M −23.58	.996	.89	5.11 (4.66–5.60)	**<.001**	2	PA
$PCSA_{MAS}$	F −22.18, M −25.36	.228	.88	5.35 (4.84–5.86)	**.001**	2	PA

Note. Bite force (BF) components, mechanical advantage, and physiological cross-sectional area (PCSA) served as dependent variables, while body mass served as the independent variable. *P* values from tests of sex effect reflect differences in elevation between the sexes, and *P* values from tests of isometry reflect differences from isometric predictions. All *P* values are reported as Benjamini-Hochberg-corrected values. Bold *P* values indicate significance ($\alpha = 0.05$). NS = nonsignificant relationship ($R^2 = 0.00–0.08$, $P = 0.067–0.680$). See table A3 for tests in difference of slopes. For scaling patterns, I = isometry, PA = positive allometry, and NA = negative allometry. f_{MAS} = masseter fiber length; f_{TEM} = temporalis fiber length; M = male; m_{MAS} = masseter mass; m_{TEM} = temporalis mass; MAM = masseter in-lever; MAT = temporalis in-lever; $masMA_C$ = masseter mechanical advantage to the canine; $masMA_M$ = masseter mechanical advantage to the molar; O_C = out-lever to canine; O_M = out-lever to molar; $PCSA_{MAS}$ = physiological cross-sectional area of masseter; $PCSA_{TEM}$ = physiological cross-sectional area of temporalis; $temMA_C$ = temporalis mechanical advantage to the canine; $temMA_M$ = temporalis mechanical advantage to the molar.

Males also exhibited significantly greater theoretical bite forces ($P < 0.001$) and larger jaw adductor muscle masses ($P < 0.001$). Despite differences in bite force, we found no significant size differences in out-lever lengths, in-lever lengths, mechanical advantage, and muscle fiber lengths ($P = 0.053–0.766$; table 6).

Discussion

Scaling of Craniomuscular Traits and Bite Force

Our study focused on measurements of body size (body mass and length), cranial measurements, and muscular traits (temporalis and master mass, fiber lengths, pennation angle, and insertion points) to understand scaling patterns in male and female southern sea otters. Our bite force model relied on the derivations of these measurements and other variables such as muscle tissue density, peak muscle stress, and gape angle for which values were taken from the literature and not directly measured.

The negative allometric relationship between body mass and condylobasal length suggests that sea otters have shorter heads in relation to their body. While this pattern is intuitive, closer examination of the scaling patterns of out-lever lengths indicates that shorter jaws may also contribute to allometric increases in theoretical bite force. The out-levers exhibit less of a positive allometric relationship compared to all the components of the bite force model. Furthermore, this allometric pattern reverses when examining the scaling relationship between out-levers and body mass; out-lever lengths are highly negatively allometric compared to all other bite force model components. Thus, these patterns strongly suggest that bite force may be partly driven by the disproportionate decreases in out-lever lengths. Theoretical bite force in southern sea otters scaled with positive allometry relative to cranial dimensions and body size through ontogeny. Studies across a broad range of taxa demonstrate that allometric increases in bite force can be attributed to allometric increase in PCSA of the jaw muscles (Pfaller et al. 2011; Kolmann et al. 2015), mechanical advantage (Grubich 2005; Huber et al. 2008), or a combination of both (Hernandez and Motta 1997; Huber et al. 2006; Kolmann and Huber 2009). In turn, allometric increases in PCSA and mechanical advantage can be achieved by changes in the underlying components:

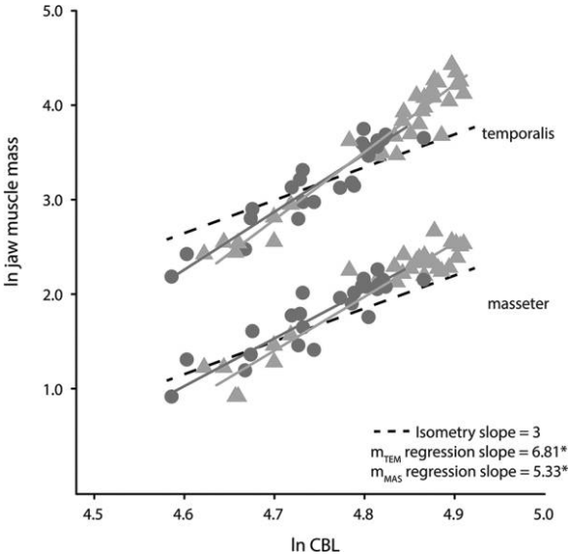

Figure 3. Scaling of temporalis (m_{TEM}) and masseter (m_{MAS}) muscle masses on condylobasal length (CBL). Circles indicate female otters, and triangles indicate male otters. Dark gray and light gray solid lines represent standardized major axis regressions for females and males, respectively. Dotted lines indicate line of isometry. An asterisk indicates that the slope is significantly different from isometry. See table 4 for more details. A color version of this figure is available online.

scaling patterns in muscle PCSA can be altered by changes in jaw muscle mass, muscle fiber lengths, and/or pennation angle (Pfaller et al. 2011; Kolmann et al. 2015), and scaling patterns of mechanical advantage can be altered by changes in in-lever and out-lever lengths (Grubich 2005; Huber et al. 2008). In sea otters, we found that positive allometry of theoretical bite force is the product of allometric increases in both muscle PCSA and mechanical advantage relative to condylobasal length. Examination of the bite force model components revealed that out-lever lengths, in-lever lengths, jaw muscle masses, and jaw muscle fiber lengths all scaled with positive allometry with respect to condylobasal length, suggesting that all these components contribute to the allometric increase in bite force. Nevertheless, CAR scores show that temporalis mass is the most important contributor to bite force estimation, indicating that ontogenetic changes in temporalis mass contributed more strongly to the ontogenetic patterns in bite force than did lever lengths or muscle fiber lengths. This is corroborated by the fact that temporalis mass was the only model component to exhibit strong positive allometry relative to body mass, suggesting that the disproportionate increase in theoretical bite force with respect to body mass is driven by the disproportionate increase in temporalis mass.

Our finding that the temporalis mass is the most important contributor to theoretical bite force is not surprising. It is well documented that the temporalis is the dominant jaw adductor muscle in carnivores (Scapino 1968; Turnbull 1970). In mustelids, the temporalis (deep and superficial) can comprise up to 80% of the jaw adductor mass (Turnbull 1970; Riley 1985; Timm 2013; Davis 2014). Large temporalis muscles are used to generate the high bite forces at large gape angles necessary to capture and kill prey (Turnbull 1970). In addition, the temporalis helps to resist dislocation of the condyle during forceful posterior biting (Maynard Smith and Savage 1959). In the durophagous southern sea otter, hard-shelled prey are often crushed with molars (carnassial position) where bite forces are greatest. Therefore, large temporalis muscles are essential in generating the high bite forces at large gape angles that are necessary to break open these heavily armored invertebrate prey (Timm 2013).

Patterns of Sexual Dimorphism

Our data indicated that adult males exhibited significantly larger cranial dimensions, bigger jaw musculature, and greater theoretical bite forces than adult females. Our finding of larger cranial traits is consistent with previous findings (Scheffer 1951; Roest 1985; Wilson et al. 1991; Law et al., forthcoming). Sexual selection may drive male sea otters to have greater biting ability than females, as they use that ability to fight with other males to defend territories (Garshelis et al. 1984) and for copulating with females, during which they grasp a female's nose with their teeth (Fisher 1939). However, a difference in absolute theoretical bite force between the sexes also is consistent with the niche divergence hypothesis, which suggests that intersexual differences in traits related to feeding are linked to dietary partitioning between the sexes (Darwin 1871; Hedrick and Temeles 1989; Shine 1989). Law et al. (forthcoming) attributed the morphological differences in the sea otter feeding apparatus as an indication of niche divergence, which also aids in the maintenance of sexual dimorphism. Southern sea otter foraging and habitat use patterns may corroborate the niche divergence hypothesis. Male sea otters utilize larger home ranges than females (Smith et al. 2015) and often are the first to explore and occupy new areas (Garshelis et al. 1984), facilitating range expansion. In addition, sea otter foraging studies in California have indicated a strong pattern of dietary specialization (Estes et al. 2003; Tinker et al. 2007), particularly in food-limited areas (Tinker et al. 2008), with females showing a greater degree of specialization (Smith et al. 2015). Generalists are typically better equipped to use a broader array of habitats and prey types (Bolnick et al. 2007; Darimont et al. 2009).Therefore, in southern sea otters, greater biting ability may benefit males as they move through and establish new territories, which may host larger or novel prey items that require greater bite force to obtain, whereas female sea otter prey diversity is constrained by their relatively small home ranges and their tendency to specialize on a few prey items. This difference may allow male sea otters to take advantage of different foraging opportunities than females and may be explained by the niche divergence hypothesis.

In contrast, when the morphological and functional traits are size corrected with either condylobasal length or body mass, we found that ontogenetic scaling patterns of cranial dimensions and theoretical bite forces do not significantly differ between the sexes, suggesting that for a given condylobasal length or body

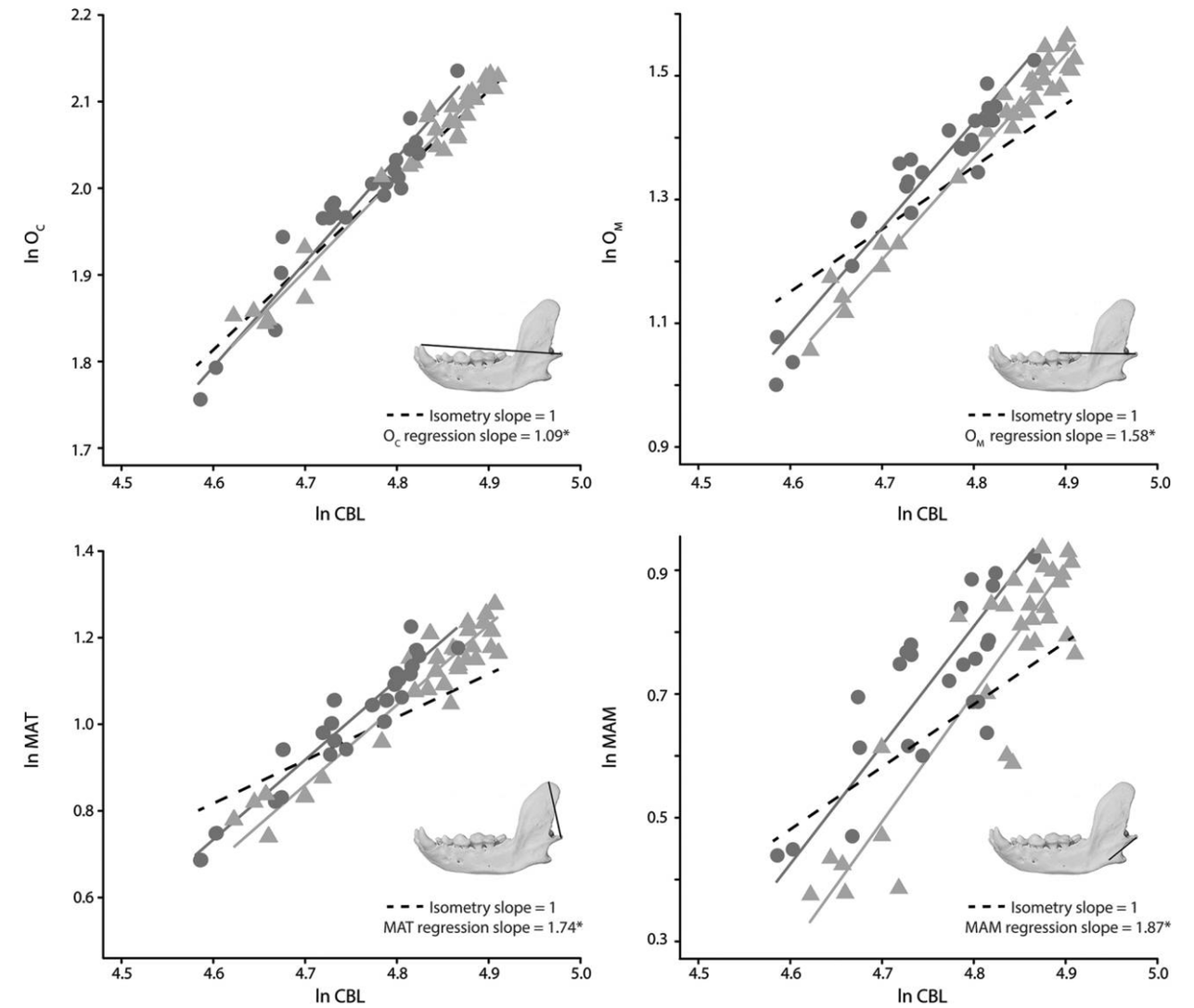

Figure 4. Scaling of out-levers and in-levers on condylobasal length. Circles indicate female otters, and triangles indicate male otters. Dark gray and light gray solid lines represent standardized major axis regressions for females and males, respectively. Dotted lines indicate line of isometry. An asterisk indicates that the slope is significantly different from isometry. See table 4 for more details. A color version of this figure is available online.

mass, males and females do not differ in cranial features related to biting or theoretical bite force. Similarly, the majority of the muscular components of our model exhibited no significant differences between the sexes when corrected for size. These results indicate that male southern sea otters exhibit greater theoretical bite forces because of their larger crania and greater jaw muscle sizes rather than differences in scaling patterns.

Despite not finding size-corrected differences in theoretical bite force between the sexes, we observed size-corrected differences in the mechanical advantage at the canine, with females exhibiting relatively higher mechanical advantage compared to males. These differences in jaw mechanics can be traced back to relative differences in lever lengths between the sexes; females exhibited relatively longer in-levers for both the temporalis and masseter muscles, whereas females and males did not exhibit relatively different canine out-lever lengths. Intersexual differences in size-corrected in-lever lengths but not size-corrected out-lever lengths are consistent with recent work based on linear measurements of 112 adult southern sea otter skulls (Law et al., forthcoming). Because higher mechanical advantage is typically associated with increased force-modified jaws (Kardong 2014), it is surprising that females exhibited relatively higher mechanical advantage than males yet did not exhibit relatively higher theoretical bite forces. A possible explanation for this observed pattern is the role of temporalis muscle mass—a trait that did not exhibit size-controlled intersexual differences—in biting performance. As the greatest contributor to bite force, temporalis muscle mass may have simply masked the signal of intersexual

Table 5: Multiple regression analyses of model components that contribute to estimated bite force

	CAR scores for BF_C components										
	O_C	MAT	MAM	m_{TEM}	m_{MAS}	f_{TEM}	f_{MAS}	Adjusted R^2	F ratio	df	P
Female	.084	.209	.073	**.392**	.210	.000	.032	1	79,730	7, 16	**<.001**
Male	.117	.168	.109	**.349**	.179	.035	.042	.99	50,240	7, 23	**<.001**
	CAR scores for BF_M components										
	O_M	MAT	MAM	m_{TEM}	m_{MAS}	f_{TEM}	f_{MAS}				
Female	.095	.210	.090	**.359**	.205	.000	.040	1	47,000	7, 13	**<.001**
Male	.111	.184	.103	**.351**	.193	.027	.032	.99	36,140	7, 15	**<.001**

Note. Correlation-adjusted correlation (CAR) scores representing relative contribution of model components to estimated bite force at the canine (BF_C) and at the molar (BF_M). Bold CAR scores represent the best model component predictor. Bold P values indicate significance ($\alpha = 0.05$). f_{MAS} = masseter fiber length; f_{TEM} = temporalis fiber length; m_{TEM} = temporalis mass; m_{MAS} = masseter mass; MAM = masseter in-lever; MAT = temporalis in-lever; O_C = out-lever to canine; O_M = out-lever to molar.

differences from mechanical advantage in our overall estimation of bite force.

Modeling Biting Ability

Our study is one of the few ontogenetic scaling studies examining the underlying muscular and skeletal components that contribute to biting ability in a single mammalian species. While the focus of our article is on the ontogenetic pattern of bite force development, our model came with two caveats. First, we were unable to empirically test our bite force model with measured bite forces from live sea otters. Southern sea otters are protected under the US Marine Mammal Protection Act as well as the US Endangered Species Act, making in vivo

Table 6: Summary statistics for raw morphological and estimated bite-force data and results of ANOVAs to assess sexual differences in each craniodental trait

Traits	Adult females ($n = 7$; mean ± SE)	Adult males ($n = 12$; mean ± SE)	$F_{1, 17}$	P
BM (kg)	17.09 ± 1.07	24.75 ± 1.31	15.0901	**.002**
BL (cm)	89.17 ± .99	97.27 ± .96	28.9562	**<.001**
CBL (cm)	123.70 ± .83	130.97 ± .97	24.3057	**<.001**
ZB (cm)	96.75 ± .63	101.79 ± 1.00	11.9562	**.004**
CH (cm)	59.30 ± .63	62.60 ± .63	11.2042	**.005**
BF_C (N)	227.73 ± 6.40	318.53 ± 12.04	27.465	**<.001**
BF_M (N)	420.48 ± 11.70	582.16 ± 19.12	33.7689	**<.001**
O_C (cm)	7.77 ± .11	8.11 ± .07	8.2809	**.013**
O_M (cm)	4.21 ± .07	4.43 ± .06	4.9634	.053
MAT (cm)	3.13 ± .05	3.21 ± .06	.848	.452
MAM (cm)	2.19 ± .07	2.33 ± .05	2.7134	.158
$temMA_C$	.40 ± .00	.40 ± .01	.7653	.455
$temMA_M$	.74 ± .01	.73 ± .01	1.9873	.225
$masMA_C$	.28 ± .01	.29 ± .01	.2967	.653
$masMA_M$	.52 ± .01	.53 ± .01	.1195	.766
m_{TEM} (g)	37.32 ± 1.03	60.64 ± 3.05	29.4098	**<.001**
m_{MAS} (g)	8.15 ± .34	10.93 ± .37	23.3904	**<.001**
f_{TEM} (cm)	4.18 ± .05	4.75 ± .13	9.295	**.010**
f_{MAS} (cm)	3.34 ± .10	3.40 ± .12	.0909	.766
$PCSA_{TEM}$ (cm^2)	8.42 ± .21	12.00 ± .45	31.5618	**<.001**
$PCSA_{MAS}$ (cm^2)	2.31 ± .10	3.07 ± .11	21.4458	**<.001**

Note. All P values are reported as Benjamini-Hochberg-corrected values. Bold P values indicate significance ($\alpha = 0.05$). BF_C = bite force at canine; BF_M = bite force at molar; BL = body length; BM = body mass; CBL = condylobasal length; CH = cranial height; f_{MAS} = masseter fiber length; f_{TEM} = temporalis fiber length; m_{MAS} = masseter mass; m_{TEM} = temporalis mass; MAM = masseter in-lever; MAT = temporalis in-lever; O_C = out-lever to canine; O_M = out-lever to molar; $PCSA_{MAS}$ = physiological cross-sectional area of masseter; $PCSA_{TEM}$ = physiological cross-sectional area of temporalis; $temMA_C$ = temporalis mechanical advantage to the canine; $temMA_M$ = temporalis mechanical advantage to the masseter; ZB = zygomatic breadth.

studies challenging. Regardless, in vivo studies would be invaluable in providing cranial and bite force measurements needed to validate our model. However, we found that our theoretical bite forces of just the adult specimens (mean adult $BF_C = 270.4$ N; mean adult $BF_M = 482.2$ N) are comparable to theoretical bite forces using the dry skull method (mean $BF_C = 281.0$ N; mean $BF_M = 394.2$ N), which uses photographs of dorsoposterior and ventral views of the cranium to estimate muscle cross-sectional area (Christiansen and Wroe 2007). In addition, our estimations of adult temporalis muscle force (310.7 N) and mass (52.6 g) and adult masseter muscle force (84.3 N) and mass (10.0 g) were similar to muscle force estimations in Alaskan sea otters (temporalis force, 313.0 N; temporalis mass, 53.6 g; and masseter force, 59.4 N; masseter mass, 7.9 g; Timm 2013). Despite our lack of in vivo bite forces, our study primarily focuses on the ontogenetic scaling of bite force generation rather than absolute values.

Second, our model does not account the force generated by the medial pterygoid, which can contribute to biting ability. However, the medial pterygoid is greatly reduced in mustelids, making up approximately 3.3% of the jaw adductor muscle volume in Alaskan sea otters (*Enhydra lutris kenyoni*; Timm 2013), 4% in ferrets (*Mustela putorius furo*; Davis 2014), and 4.2% in Eurasian otters (*Lutra lutra*; Turnbull 1970). Because of its relatively small size, the medial pterygoid is a weak adductor and more likely serves in stabilizing the jaws during biting in mustelids (Davis 2014). Estimation of medial pterygoid force generation (19.5 N) accounted for just 4.9% of total jaw muscle force generation in Alaskan sea otters (Timm 2013). Therefore, the medial pterygoid is unlikely to significantly contribute to biting ability.

Conclusion

We found that in southern sea otters, allometric increases of PCSA for the major jaw adductor muscle and mechanical advantage underlie the pattern of positive allometry for theoretical bite force. Although all the components of our model scaled with positive allometry relative to condylobasal length, CAR scores indicated that temporalis muscle mass was the greatest contributor to theoretical bite force. This is corroborated by the fact that temporalis mass was the only model component out of eight variables to exhibit positive allometry relative to body mass. Alternatively, allometric decreases in out-lever lengths also contribute to allometric increases in theoretical bite force. In our analysis of sexual dimorphism, we found no differences in scaling patterns of bite force and morphological traits between the sexes through ontogeny. Although we did not find size-corrected differences in theoretical bite forces, muscle PCSA, and the majority of cranial traits between the sexes, we found that for a given condylobasal length or body mass, female sea otters exhibit relatively longer temporalis and masseter in-levers but shorter molar out-levers. We postulate that as the greatest contributor to theoretical bite force, temporalis muscle mass may have masked the signal of sex effects from lever lengths in our overall estimation of bite force. In adults, we found that adult male sea otters can generate greater bite forces than adult female sea otters, and these intersexual differences are a result of differences in overall size (in which males are larger) rather than differences in scaling patterns. Our results demonstrating a difference in absolute theoretical bite force between the sexes are consistent with the niche divergence hypothesis. Nevertheless, additional field studies in sea otter foraging ecology will further validate the role of the niche divergence hypothesis in the maintenance of sexual dimorphism in sea otters.

Acknowledgments

We are grateful to Erin Dodd (California Department of Fish and Wildlife [CDFW]), Francesca Batac (CDFW), and Sue Pemberton (California Academy of Sciences) for helping clean out the skulls; Lilian Carswell (US Fish and Wildlife Service) for permitting logistics; Tim Tinker (US Geological Survey) for helpful discussions on sea otter life history; Sharlene Santana (University of Washington) for providing PDFs of rare references; and Vikram Baliga (University of California–Santa Cruz) for guidance with the statistical analyses. We also thank Vikram Baliga, Ben Higgins, Jacob Harrison, and two anonymous reviewers for helpful comments and discussions on various versions of this manuscript. Funding was provided partly by a Grant-in-Aid of Research from the American Society of Mammalogists, a Lerner-Gray Fund through the American Museum of Natural History, a Rebecca and Steve Sooy Graduate Research Fellowship for Marine Mammals, and a National Science Foundation Graduate Research Fellowship (all awarded to C.J.L.).

APPENDIX

Supplementary Tables

Table A1: Specimens used in this study

Female			Male		
CDFW specimen no.	Body mass (kg)	Body length (cm)	CDFW specimen no.	Body mass (kg)	Body length (cm)
6859-13	22.5	88.5	6857-13	27.1	99
6977-13	7	73.5	6914-13	20.5	95
7039-14	11.8	82	6919-13	24.1	93
7075-14	12.8	80	7022-14	20	98
7138-14	20.6	92.5	7078-14	18.8	92
7157-14	6.465	64.5	7136-14	6.175	58
7171-14	13.2	89.5	7207-14	33.4	102.5
7205-14	12.6	89	7216-14	32.8	101
7232-14	16.2	85	7272-14	14	83
7248-14	4.64	56	7294-14	17.1	100
7268-14	5.5	60.5	7301-14	16.9	87
7276-14	15.6	80	7302-14	16.1	88.5
7285-14	7	72	7310-14	6.36	63
7382-14	14.1	80.5	7318-14	21	91
7634-15	8.8	67	7322-14	22.2	100
7637-15	16.9	93	7342-14	25.7	98.6
7645-15	10.9	77	7391-14	8.2	71.5
7657-15	8.7	73	7405-15	16	81.5
7666-15	16.2	92	7415-15	6	59.5
7668-15	17.1	88	7503-15	13.34	77.5
7744-15	11.2	75	7529-15	31	94
7749-15	19.1	88	7626-15	29.7	92
7774-15	16.5	85	7665-15	9.4	71
7777-16	8.5	74	7743-15	9.9	68
			7752-15	24.6	98
			7755-15	13.3	99
			7758-15	6	65
			7763-15	20.6	96
			7764-15	20.1	96
			7773-15	24.9	98
			7789-16	30.8	104

Note. CDFW = California Department of Fish and Wildlife.

Table A2: Age classes of the southern sea otter and the skull sample size per age class used in this study

Age class	Age	Skull sample size	Total body length (cm)	Skull characteristics
Pup	2.5–6 mo	F 2, M 1	40–90	All sutures open; all teeth deciduous
Immature	6 mo–1 yr	F 5, M 6	80–105	Exoccipital-basioccipital suture closed; some teeth deciduous, some permanent
Subadult	1–4 yr	F 8, M 7	F 95–115, M 100–125	Basioccipital-basisphenoid suture open; all teeth permanent; no tooth wear evident
Adult	4–9 yr	F 9, M 17	F > 105, M > 115	All sutures closed; lambdoidal and sagittal crests starting to develop; slight to obvious tooth wear

Note. Age classes were defined based on the total body length and skull characteristics following California Department of Fish and Wildlife protocol (Hatfield 2006). F = female; M = male.

Table A3: Comparison of the mean slopes between the sexes

Dependent variable	Mean slopes	*t*	df	*P*
Cranial dimensions against BM:				
CBL	F .17, M .17	2.85E-05	1	.996
ZB	F .19, M .18	.352	1	.553
CH	F .10, M .12	1.28	1	.258
Cranial dimensions against BL:				
CBL	F .52, M .50	.147	1	.701
ZB	F .60, M .55	1.116	1	.291
CH	F .30, M .38	.8802	1	.348
BF_C against body and cranial dimensions:				
BM	F .84, M .96	1.624	1	.203
BL	F 2.63, M 2.92	.976	1	.323
CBL	F 5.05, M 5.79	1.709	1	.204
ZB	F 4.37, M 5.33	3.945	1	.052
CH	F 8.63, M 7.85	.198	1	.635
BF_M against body and cranial dimensions:				
BM	F .79, M .88	1.055	1	.304
BL	F −2.49, M −2.69	.5526	1	.457
CBL	F 4.77, M 5.32	1.002	1	.317
ZB	F 4.13, M 4.90	2.649	1	.104
CH	F 8.17, M 7.22	.3348	1	.563
BF components against CBL:				
O_C	F 1.20, M 1.09	2.006	1	.157
O_M	F 1.62, M 1.63	.008438	1	.927
MAT	F 1.93, M 1.80	.6233	1	.430
MAM	F 1.85, M 2.10	.661	1	.416
m_{TEM}	F 12.24, M 14.32	2.786	1	.095
m_{MAS}	F 5.04, M 5.69	1.143	1	.285
f_{TEM}	F 2.40, M 2.13	.3868	1	.534
f_{MAS}	F 2.05, M 1.93	.08146	1	.775
MA against CBL:				
$temMA_C$	F .83, M .83	2.66E-06	1	.999
$temMA_M$				
$masMA_C$	F 1.08, M 1.25	.3395	1	.560
$masMA_M$				
PCSA against CBL:				
$PCSA_{TEM}$	F 4.62, M 5.34	1.762	1	.184
$PCSA_{MAS}$	F −5.04, M −5.69	1.143	1	.285
BF components against BM:				
O_C	F .20, M .18	.7311	1	.393
O_M	F .27, M .27	.003539	1	.953
MAT	F .32, M .30	.3245	1	.569
MAM	F .31, M .35	.4502	1	.502
m_{TEM}	F 1.02, M 1.19	2.276	1	.131
m_{MAS}	F .84, M .95	.8881	1	.346
f_{TEM}	F .40, M .35	.352	1	.553
f_{MAS}	F .34, M .32	.0793	1	.778
MA against BM:				
$temMA_C$	F .14, M .14	2.17E-05	1	.996
$temMA_M$				
$masMA_C$	F .18, M .21	.2424	1	.623
$masMA_M$				
PCSA against BM:				
$PCSA_{TEM}$	F .77, M .89	1.827	1	.177
$PCSA_{MAS}$	F .84, M .95	.8881	1	.431

Note. The trait listed in each row indicates the dependent variable used in sex-specific standardized major axis regressions. *P* values are reported as Benjamini-Hochberg-corrected values. Significance level = 0.05. BL = body length; BM = body mass; CBL = condylobasal length; CH = cranial height; F = female; f_{MAS} = masseter fiber length; f_{TEM} = temporalis fiber length; M = male; m_{MAS} = masseter mass; m_{TEM} = temporalis mass; MAM = masseter in-lever; MAT = temporalis in-lever; O_C = out-lever to canine; O_M = out-lever to molar; $PCSA_{TEM}$ = physiological cross-sectional area of temporalis; $PCSA_{MAS}$ = physiological cross-sectional area of masseter; $temMA_C$ = temporalis mechanical advantage to the canine; $temMA_M$ = temporalis mechanical advantage to the masseter; ZB = zygomatic breadth.

Table A4: Scaling of bite force model components (pt. A), mechanical advantage (pt. B), and physiological cross-sectional area (pt. C) against body mass

	Sex effects		Scaling relationships				
	Intercept	*P*	R^2	Slope (95% CI)	*P*	Isometric prediction	Scaling patterns
A. BF components against BM:							
O_C	F 1.49, M 1.53	.515	.86	.18 (.17–.21)	**<.001**	.33	NA
O_M	F .69, M .64	**.047**	.82	.26 (.24–.3)	**.001**	.33	NA
MAT	F .23, M .24	**.040**	.81	.29 (.26–.33)	**.041**	.33	NA
MAM	F −.05, M −.25	**.004**	.63	.31 (.26–.37)	.408	.33	I
m_{TEM}	F .71, M .30	.761	.9	1.15 (1.05–1.25)	**.041**	1	PA
m_{MAS}	F −.25, M −.58	.663	.84	.9 (.8–.99)	**.047**	1	NA
f_{TEM}	F .35, M .44	.774	.62	.38 (.31–.46)	.183	.33	I
f_{MAS}	F .26, M .23	.089	.36	.31 (.24–.4)	.578	.33	I
B. MA against BM:							
$temMA_C$	F −1.31, M −1.35	**.009**	.53	.13 (.10–.15)	**<.001**	0	PA
$temMA_M$				NS			
$masMA_C$	F −1.71, M −1.88	**.001**	.19	.18 (.13–.23)	**<.001**	0	PA
$masMA_M$				NS			
C. PCSA against BM:							
$PCSA_{TEM}$	F −.07, M −.34	.663	.88	.86 (.78–.95)	**<.001**	.67	PA
$PCSA_{MAS}$	F −.25, M −.57	.663	.84	.9 (.80–1.00)	.198	.67	I

Note. Bite force components, mechanical advantage, and physiological cross-sectional area served as dependent variables, while body mass served as the independent variable. *P* values from tests of sex effect reflect differences in elevation between the sexes, and *P* values from tests of isometry reflect differences from isometric predictions. All *P* values are reported as Benjamini-Hochberg-corrected values. Bold *P* values indicate significance ($\alpha = 0.05$). NS = nonsignificant relationship ($R^2 = 0.00–0.10$, $P = 0.067–0.561$). See table A3 for tests in difference of slopes. CI = confidence interval. For scaling patterns, I = isometry, NA = negative allometry, and PA = positive allometry. F = female; f_{MAS} = masseter fiber length; f_{TEM} = temporalis fiber length; M = male; m_{MAS} = masseter mass; m_{TEM} = temporalis mass; MAM = masseter in-lever; $masMA_C$ = masseter mechanical advantage to the canine; $masMA_M$ = masseter mechanical advantage to the molar; MAT = temporalis in-lever; O_C = out-lever to canine; O_M = out-lever to molar; $PCSA_{MAS}$ = physiological cross-sectional area of masseter; $PCSA_{TEM}$ = physiological cross-sectional area of temporalis; $temMA_C$ = temporalis mechanical advantage to the canine; $temMA_M$ = temporalis mechanical advantage to the molar.

Table A5: Multiple regression analyses of model components that contribute to estimated bite force

	CAR scores for BF_C components									
	$temMA_C$	$masMA_C$	m_{TEM}	m_{MAS}	f_{TEM}	f_{MAS}	Adjusted R^2	*F* ratio	df	*P*
Female	.215	.024	**.469**	.264	.000	.026	1	10,960	6, 17	**<.001**
Male	.127	.070	**.428**	.254	.064	.058	1	51,660	6, 24	**<.001**
	CAR scores for BF_M components									
	$temMA_M$	$masMA_M$	m_{TEM}	m_{MAS}	f_{TEM}	f_{MAS}				
Female	.078	.001	**.557**	.328	.000	.035	1	9,277	6, 17	**<.001**
Male	.018	.016	**.517**	.308	.077	.064	1	41,240	6, 24	**<.001**

Note. Correlation-adjusted correlation (CAR) scores representing relative contribution of model components to estimated bite force at the canine (BF_C) and at the molar (BF_M). Bold CAR scores represent the best model component predictor. Bold *P* values indicate significance ($\alpha = 0.05$). f_{MAS} masseter fiber length; f_{TEM} = temporalis fiber length; m_{MAS} = masseter mass; m_{TEM} = temporalis mass; $temMA_C$ = temporalis mechanical advantage to the canine; $temMA_M$ = temporalis mechanical advantage to the masseter.

Literature Cited

Anderson R.A., L.D. McBrayer, and A. Herrel. 2008. Bite force in vertebrates: opportunities and caveats for use of a nonpareil whole-animal performance measure. Biol J Linn Soc 93:709–720.

Baliga V.B. and R.S. Mehta. 2014. Scaling patterns inform ontogenetic transitions away from cleaning in *Thalassoma* wrasses. J Exp Biol 217:3597–3606.

Benjamini Y. and Y. Hochberg. 1995. Controlling the false discovery rate: a practical and powerful approach to multiple testing. J R Stat Soc B 57:289–300.

Biewener A.A. and R.J. Full. 1992. Force platform and kinematic analysis. Pp. 45–73 in A.A. Biewener, ed. Biomechanics structures and systems: a practical approach. Oxford University Press, New York.

Binder W.J. and B. Valkenburgh. 2000. Development of bite strength and feeding behaviour in juvenile spotted hyenas (*Crocuta crocuta*). J Zool 252:273–283.

Bolnick D.I., P. Amarasekare, M.S. Araújo, R. Bürger, J.M. Levine, M. Novak, V.H.W. Rudolf, et al. 2011. Why intraspecific trait variation matters in community ecology. Trends Ecol Evol 26:183–192.

Bolnick D.I., R. Svanbäck, M.S. Araújo, and L. Persson. 2007. Comparative support for the niche variation hypothesis that more generalized populations also are more heterogeneous. Proc Natl Acad Sci USA 104:10075–10079.

Bulté G., D.J. Irschick, and G. Blouin-Demers. 2008. The reproductive role hypothesis explains trophic morphology dimorphism in the northern map turtle. Funct Ecol 22:824–830.

Camilleri C. and R. Shine. 1990. Sexual dimorphism and dietary divergence: differences in trophic morphology between male and female snakes. Copeia 1990:649–658.

Christiansen P. and S. Wroe. 2007. Bite forces and evolutionary adaptations to feeding ecology in carnivores. Ecology 88: 347–358.

Clutton-Brock T. 2007. Sexual selection in males and females. Science 318:1882–1885.

Collar D.C., J.S. Reece, M.E. Alfaro, and P.C. Wainwright. 2014. Imperfect morphological convergence: variable changes in cranial structures underlie transitions to durophagy in moray eels. Am Nat 183:E168–E184. doi:10.1086/675810.

Constantino P.J., J.J.W. Lee, D. Morris, P.W. Lucas, A. Hartstone-Rose, W.-K. Lee, N.J. Dominy, et al. 2011. Adaptation to hard-object feeding in sea otters and hominins. J Hum Evol 61:89–96.

Darimont C.T., P.C. Paquet, and T.E. Reimchen. 2009. Landscape heterogeneity and marine subsidy generate extensive intrapopulation niche diversity in a large terrestrial vertebrate. J Anim Ecol 78:126–133.

Darwin C. 1871. The descent of man and selection in relation to sex. J. Murray, London.

Davis J.L., S.E. Santana, E.R. Dumont, and I.R. Grosse. 2010. Predicting bite force in mammals: two-dimensional versus three-dimensional lever models. J Exp Biol 213:1844–1851.

Davis J.S. 2014. Functional morphology of mastication in musteloid carnivorans. PhD diss. Ohio State University, Columbus.

Emerson S.B. and D.M. Bramble. 1993. Scaling, allometry, and skull design. Pp. 384–421 in J. Hanken and B.K. Hall, eds. The skull. Vol. 3. Functional and evolutionary mechanisms. University of Chicago Press, Chicago.

Erickson G.M., A.K. Lappin, and K.A. Vliet. 2003. The ontogeny of bite-force performance in American alligator (*Alligator mississippiensis*). J Zool 260:317–327.

Estes J.A., M.L. Riedman, M.M. Staedler, M.T. Tinker, and B.E. Lyon. 2003. Individual variation in prey selection by sea otters: patterns, causes and implications. J Anim Ecol 72:144–155.

Fisher E.M. 1939. Habits of the southern sea otter. J Mammal 20:21.

———. 1941. Notes on the teeth of the sea otter. J Mammal 22:428.

Garshelis D.L. and A.M. Johnson. 1984. Social organization of sea otters in Prince William Sound, Alaska. Can J Zool 62: 2648–2658.

Grömping U. 2006. Relative importance for linear regression in R: the package relaimpo. J Stat Softw 17:1–27.

Grubich J.R. 2005. Disparity between feeding performance and predicted muscle strength in the pharyngeal musculature of black drum, *Pogonias cromis* (Sciaenidae). Environ Biol Fish 74:261–272.

Hatfield B. 2006. Protocol for stranded and dead sea otters. California Department of Fish and Wildlife, Sacramento.

Hedrick A.V. and E.J. Temeles. 1989. The evolution of sexual dimorphism in animals: hypotheses and tests. Trends Ecol Evol 4:136–138.

Hernandez L.P. and P.J. Motta. 1997. Trophic consequences of differential performance: ontogeny of oral jaw-crushing performance in the sheepshead, *Archosargus probatocephalus* (Teleostei, Sparidae). J Zool 243:737–756.

Herrel A., R.V. Damme, B. Vanhooydonck, and F.D. Vree. 2001. The implications of bite performance for diet in two species of lacertid lizards. Can J Zool 79:662–670.

Herrel A., A. De Smet, L.F. Aguirre, and P. Aerts. 2008. Morphological and mechanical determinants of bite force in bats: do muscles matter? J Exp Biol 211:86–91.

Herrel A., R. Joachim, B. Vanhooydonck, and D.J. Irschick. 2006. Ecological consequences of ontogenetic changes in head shape and bite performance in the Jamaican lizard *Anolis lineatopus*. Biol J Linn Soc 89:443–454.

Herrel A., L.D. McBrayer, and P.M. Larson. 2007. Functional basis for sexual differences in bite force in the lizard *Anolis carolinensis*. Biol J Linn Soc 91:111–119.

Herrel A., L. Spithoven, R. Van Damme, and F. De Vree. 1999. Sexual dimorphism of head size in *Gallotia galloti*: testing the niche divergence hypothesis by functional analyses. Funct Ecol 13:289–297.

Herzog W. 1994. Muscle. Pp. 154–187 in B.M. Nigg and W. Herzog, eds. Biomechanics of the musculoskeletal system. Wiley, Chichester.

Hill A.V. 1950. The dimensions of animals and their muscular dynamics. Sci Prog 38:209–230.

Huber D.R., M.N. Dean, and A.P. Summers. 2008. Hard prey, soft jaws and the ontogeny of feeding mechanics in the spotted ratfish *Hydrolagus colliei*. J R Soc Interface 5:941–952.

Huber D.R., C.L. Weggelaar, and P.J. Motta. 2006. Scaling of bite force in the blacktip shark *Carcharhinus limbatus*. Zoology 109:109–119.

Kardong K.V. 2014. Vertebrates: comparative anatomy, function, evolution. McGraw-Hill, Boston.

Kolmann M.A. and D.R. Huber. 2009. Scaling of feeding biomechanics in the horn shark *Heterodontus francisci*: ontogenetic constraints on durophagy. Zoology 112:351–361.

Kolmann M.A., D.R. Huber, P.J. Motta, and R.D. Grubbs. 2015. Feeding biomechanics of the cownose ray, *Rhinoptera bonasus*, over ontogeny. J Anat 227:341–351.

Law C.J., V. Venkatram, and R.S. Mehta. Forthcoming. Sexual dimorphism in the craniomandibular morphology of southern sea otters (*Enhydra lutris nereis*). J Mammal.

Marshall C.D., A. Guzman, T. Narazaki, K. Sato, E.A. Kane, and B.D. Sterba-Boatwright. 2012. The ontogenetic scaling of bite force and head size in loggerhead sea turtles (*Caretta caretta*): implications for durophagy in neritic, benthic habitats. J Exp Biol 215:4166–4174.

Marshall C.D., J. Wang, A. Rocha-Olivares, C. Godinez-Reyes, S. Fisler, T. Narazaki, K. Sato, et al. 2014. Scaling of bite performance with head and carapace morphometrics in green turtles (*Chelonia mydas*). J Exp Mar Biol 451:91–97.

Maynard Smith J. and R. Savage. 1959. The mechanics of mammalian jaws. Sch Sci Rev 141:289–301.

McGee M.D. and P.C. Wainwright. 2013. Sexual dimorphism in the feeding mechanism of threespine stickleback. J Exp Biol 216:835–840.

Mendez J. and A. Keys. 1960. Density and composition of mammalian muscle. Metab Clin Exp 9:184–188.

Pfaller J.B., P.M. Gignac, and G.M. Erickson. 2011. Ontogenetic changes in jaw-muscle architecture facilitate durophagy in the turtle *Sternotherus* minor. J Exp Biol 214:1655–1667.

R Core Team. 2015. R: a language and environment for statistical computing. R Foundation for Statistical Computing, Vienna. http://www.R-project.org/.

Radford A.N. and M.A. Du Plessis. 2003. Bill dimorphism and foraging niche partitioning in the green woodhoopoe. J Anim Ecol 72:258–269.

Riedman M. and J.A. Estes. 1990. The sea otter (*Enhydra lutris*): behavior, ecology, and natural history. Biol Rep 90:1–117.

Riley M.A. 1985. An analysis of masticatory form and function in three mustelids (*Martes americana, Lutra canadensis, Enhydra lutris*). J Mammal 66:519–528.

Roest A.I. 1985. Determining the sex of sea otters from skulls. Calif Fish Game 71:179–183.

Sacks R.D. and R.R. Roy. 1982. Architecture of the hind limb muscles of cats: functional significance. J Morphol 173:185–195.

Santana S.E., E. Dumont, and J.L. Davis. 2010. Mechanics of bite force production and its relationship to diet in bats. Funct Ecol 24:776–784.

Santana S.E. and K.E. Miller. 2016. Extreme postnatal scaling in bat feeding performance: a view of ecomorphology from ontogenetic and macroevolutionary perspectives. Integr Comp Biol. doi:10.1093/icb/icw075.

Scapino R.P. 1968. Biomechanics of feeding in Carnivora. PhD diss. University of Illinois, Chicago.

Scheffer V.B. 1951. Measurements of sea otters from western Alaska. J Mammal 32:10–14.

Schmidt-Nielsen K. 1984. Scaling. Cambridge University Press, Cambridge.

Schneider C.A., W.S. Rasband, and K.W. Eliceiri. 2012. NIH Image to ImageJ: 25 years of image analysis. Nat Methods 9: 671–675.

Shine R. 1989. Ecological causes for the evolution of sexual dimorphism: a review of the evidence. Q Rev Biol 64:419–461.

Smith E.A., S.D. Newsome, J.A. Estes, and M.T. Tinker. 2015. The cost of reproduction: differential resource specialization in female and male California sea otters. Oecologia 178: 17–29.

Thom M.D. and L.A. Harrington. 2004. Why are American mink sexually dimorphic? a role for niche separation. Oikos 105:525–535.

Thomas P., E. Pouydebat, I. Hardy, F. Aujard, C.F. Ross, and A. Herrel. 2015. Sexual dimorphism in bite force in the grey mouse lemur. J Zool 296:133–138.

Timm L.L. 2013. Feeding biomechanics and craniodental morphology in otters (Lutrinae). PhD diss. Texas A&M University, College Station.

Timm-Davis L.L., T.J. DeWitt, and C.D. Marshall. 2015. Divergent skull morphology supports two trophic specializations in otters (Lutrinae). PLoS ONE 10:e0143236.

Tinker M.T., G. Bentall, and J.A. Estes. 2008. Food limitation leads to behavioral diversification and dietary specialization in sea otters. Proc Natl Acad Sci USA 105:560–565.

Tinker M.T., D.P. Costa, J.A. Estes, and N. Wieringa. 2007. Individual dietary specialization and dive behaviour in the California sea otter: using archival time-depth data to detect alternative foraging strategies. Deep Sea Res II 54: 330–342.

Turnbull W.D. 1970. Mammalian masticatory apparatus. Field Museum of Natural History, Chicago.

van der Meij M.A.A. and R.G. Bout. 2006. Seed husking time and maximal bite force in finches. J Exp Biol 209:3329–3335.

Van Valkenburgh B. 2007. Deja vu: the evolution of feeding morphologies in the Carnivora. Am Zool 47:147–163.

Verwaijen D., R. Van Damme, and A. Herrel. 2002. Relationships between head size, bite force, prey handling efficiency and diet in two sympatric lacertid lizards. Funct Ecol 16: 842–850.

Warton D.I., R.A. Duursma, D.S. Falster, and S. Taskinen. 2011. smatr 3: an R package for estimation and inference about allometric lines. Methods Ecol Evol 3:257–259.

Wilson D.E., M.A. Bogan, R.L. Brownell, A.M. Burdin, and M.K. Maminov. 1991. Geographic variation in sea otters, *Enhydra lutris*. J Mammal 72:22–36.

Ziscovici C., P.W. Lucas, P.J. Constantino, T.G. Bromage, and A. van Casteren. 2014. Sea otter dental enamel is highly resistant to chipping due to its microstructure. Biol Lett 10: 20140484.

Zuber V. and K. Strimmer. 2011. High-dimensional regression and variable selection using CAR scores. Stat Appl Genet Mol Biol 10:1–34.